APPLIED
MATERIALS
AND TECHNOLOGY

Research Article

Jamt.ejournal.unri.ac.id

Photo-Fenton of Dyes Degradation Using Covalent Triazine Frameworks: Towards Industrial Wastewater Treatment Applications

Barata Aditya Prawiranegara[1*], Heni Sugesti[2], Suhendri[3], Hussein Rasool Abid[4,5,6], Muhammad Rizwan Azhar[4], Zana Hassan Rada[4], Maykel Manawan[7], Panca Setia Utama[3]

[1]Department of Chemistry, Faculty of Mathematics and Natural Sciences, Universitas Riau, Pekanbaru, 28293, Indonesia
[2]Department of Chemical Engineering, Politeknik Negeri Sriwijaya, Palembang, 30128, Indonesia
[3]Department of Chemical Engineering, Universitas Riau, Pekanbaru 28293, Indonesia
[4]School of Engineering, Edith Cowan University, 270 Joondalup Dr, Joondalup 6027 WA, Australia
[5]Centre for Sustainable Energy and Resources, Edith Cowan University, 270 Joondalup Drive, Joondalup 6027 WA, Australia
[6]Environmental Health Department, Applied Medical Sciences, University of Karbala, Karbala 56001, Iraq
[7]Fakultas Teknologi Pertahanan, Universitas Pertahanan Indonesia, Jawa Barat 16810, Indonesia

ABSTRACT: A Covalent Triazine Framework (CTF-1) and carbon nanospheres (CS) were synthesized to develop a porous, thermally stable, and efficient photocatalyst for dye degradation in wastewater treatment applications. The synthesized composite material exhibited a high surface area exceeding 400 m^2/g, a well-defined mesoporous structure, and excellent optical properties, including strong light absorption extending up to 550 nm and a moderate band gap of approximately 2.8 eV. These characteristics promote effective visible light-driven photocatalysis. The photocatalytic performance was assessed by degrading methylene blue (MB) as a model organic dye pollutant under photo-Fenton conditions. The system demonstrated high efficiency, with over 90% of the dye removed within 120 minutes of irradiation. The degradation followed pseudo-first-order kinetics, confirming the photocatalytic nature of the reaction. Parameter studies indicated that hydroxyl radicals (•OH) were the dominant reactive species responsible for dye degradation. Moreover, CTF-1 retained its photocatalytic activity and structural integrity over multiple reuse cycles, showcasing excellent reusability and stability. The integration of high surface area for dye adsorption, efficient photoactivation under visible light, and robust radical generation synergistically contributed to the enhanced degradation performance. The study highlights the promising role of CTF-1 and its composites as multifunctional materials for advanced oxidation processes. Given its effectiveness, durability, and environmental compatibility, CTF-1 presents a sustainable and scalable solution for the treatment of dye-laden industrial wastewater. This work contributes to the development of next-generation photocatalysts aimed at addressing global challenges in water pollution and environmental remediation

Key words: Covalent triazine framework, photo-Fenton, methylene blue, photocatalysis, wastewater treatment.

1. INTRODUCTION

Dyes are considered crucial in various industries such as textiles, cosmetics, and food processing, leading to a significant annual production estimated at around 700,000 tons globally, which includes approximately 10,000 different pigments [1]. This large-scale production has raised concerns regarding environmental pollution, given that a notable percentage of these dyes are discharged into wastewater during dyeing processes [2]. Textile wastewater, known for containing a variety of pollutants ranging from dyes to toxic organic compounds represents a critical environmental challenge impacting aquatic ecosystems [3].

The classification of dyes is based on their chemical structures, which include groups like azo, xanthene, and thiazine [4]. In particular, xanthene dyes, such as Rhodamine B, and thiazine dyes like Methylene Blue, are selected for this study due to their widespread use and persistent toxicity, which complicates efforts for their biodegradation and removal from wastewater [5, 6]. The substantial ecological ramifications of these dyes necessitate effective removal methods as they can hinder light penetration in water bodies, thus affecting aquatic life [7].

The health implications of dye exposure are notable, with several studies indicating that many textile dyes possess carcinogenic or allergenic properties leading to skin irritation and dermatitis [6]. Therefore, mitigating the discharge of these dyes into water bodies is crucial for ecological well-being and public health [3]. Conventional methods for dye removal, such as coagulation and flocculation, tend to produce secondary waste [8]. While

Received : July 07, 2025
Revised : August 07, 2025
Accepted : August 10, 2025

biological treatment methods may be economically favorable, they often prove ineffective against complex dye structures [9]. Therefore, advanced oxidation processes (AOPs) like Fenton and photo-Fenton methods have gained attention for their potential to mineralize persistent organic pollutants effectively [3].

Processes such as Fenton and photo-Fenton utilize hydroxyl radicals generated in situ from hydrogen peroxide and ferrous ions to oxidize a variety of organic contaminants [10]. Fenton's reaction, characterized by the oxidation of ferrous ions to ferric ions, facilitates a cycle wherein the generated radicals play a crucial role in degrading organic pollutants into benign by-products [11]. In the photo-Fenton process, the introduction of light enhances the generation of hydroxyl radicals, thus accelerating the degradation process [12]. Numerous studies have corroborated the effectiveness of the photo-Fenton process for specific dyes, achieving substantial removal efficiencies under optimal conditions [13].

The experimental section of this study investigates the efficiency of Fenton and photo-Fenton processes for degrading Methylene Blue using CTF-1 and CS. While previous studies have explored various photocatalysts for dye degradation, limited research has focused on the use of Covalent Triazine Frameworks (CTFs) combined with carbon nanostructures under photo-Fenton conditions. The research gap lies in the lack of efficient, reusable, and metal-free photocatalysts that operate effectively under visible light. This study addresses that gap by developing a CTF-1/CS composite, aiming to enhance light absorption, charge separation, and hydroxyl radical generation. The novelty of this work lies in the integration of adsorption, photocatalysis, and Fenton-like activity into a single, stable material designed for sustainable industrial wastewater treatment.

2. MATERIAL AND METHODS

2.1 Photocatalyst preparations

CTF-1 was prepared by a modified ionothermal method as shown in Figure 1 Dicyanobenzene (DCB) 1 g (0.0078 mol) mixed with a 5 g of $ZnCl_2$. The mixture was then heated in a furnace with an argon atmosphere for 24 hours at a temperature of 400°C. The product is then washed many times with HCl, ethanol, then distilled water. After that, the material was dried in an oven at 90 °C for 12 hours. For CS synthetic process, Typically, 7.24 g (0.02 mol) of honey was dissolved in 50 mL of distilled water. Furthermore, 97% ammonia was added until the pH of the solution reached 10. After stirring, the solution was put into a Teflon-lined autoclave and heated for 18 h at 180 °C. The autoclave was cooled down to room temperature, and the precipitated materials were filtered and washed using water. Then the precipitate was dried at 120 °C for three h and then calcined at 550 °C in argon for 4 h. The solid product was referred to as the carbon nanosphere (CS).

2.2 Photocatalytic processes

A total of 250 ml of 20 ppm MB solution was put into the 1000 mL reactor and the catalyst were added as much as 0.125 g (500mg/L) then the mixture was stirred with a stirrer. The solution was left without irradiation for 40 minutes for adjusting the adsorption equilibrium. After that, the solution was irradiated with a Mercury UV-Vis lamp λ = 350 nm for 2 hours. The solution was taken with 1 mL syringe and filtered out every 10 minutes. Then the solution is tested for concentration using a UV-Vis spectrometer. Variables such as Catalyst variants, effects of MB concentration, oxidant, scavenger, and catalyst reusability were also tested in this study.

2.3 Catalyst characterization

The surface morphologies, compositions, and functional groups were analyzed with FE-SEM/EDX (Field Emission Scanning Electron Microscopy/Energy-dispersive X-ray) using Zeiss EVOLS15, XPS (X-ray Photoelectron Spectrometer) using Thermo Scientific K-Alpha and image J software for length measurement, and KBr method FTIR (Fourier Transform Infrared Spectroscopy) using Thermoscientific Nicolet iS-10 with range 400–4000 cm^{-1}. The isotherm and surface area BET (Brunauer Emmett Teller) analysis was performed using Micromeritics Tristar 3000. The crystallinity of the as-prepared sample was analyzed using XRD (X-ray Diffractometer) PANalytical AERIS with Cu Kα irradiation (λ = 1.54) range, 0° with a step size of 2°/step and exposure time of 1 s/step. The UV–vis DRS (Diffuse Reflection Spectroscopy) was analyzed using Shimadzu UV-2600i with a wavelength of 200–800 nm.

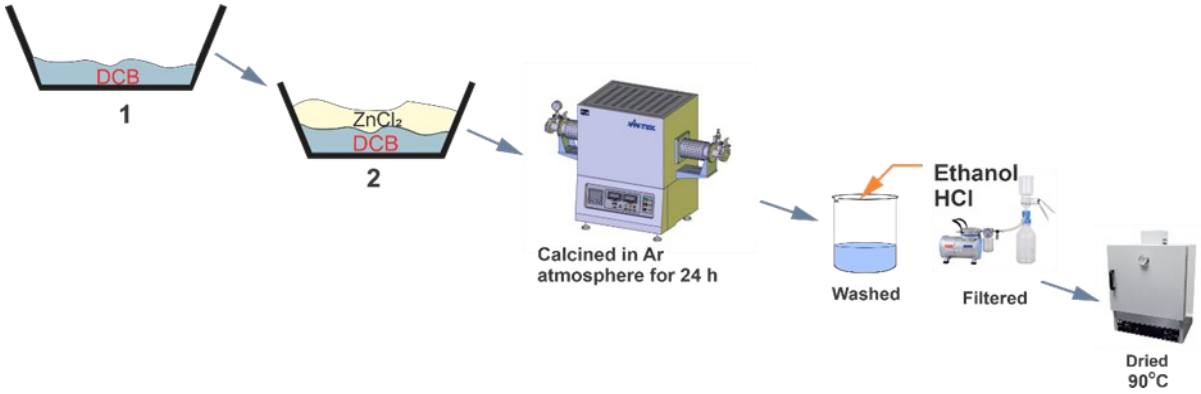

Fig. 1. Ionothermal synthesis method of CTF-1

3. RESULT AND DISCUSSION

Mechanism of synthetic of the CTFs-1 as shown on the Figure 2, the molten $ZnCl_2$ in ionothermal process, act as a Lewis acid that will accept an electron pair from 1,4-dicyanobenzene (DCB) (1) This process will activate DCB nitrile group which makes the trimerization process would occur [14] (2 - 4). As the trimerization process finished, the CTF-1 was successfully synthesized. The CS on the other hands, hydrothermal reaction was used. Hydrothermal utilize honey that solved in water then superheated at 180 ^{O}C. Superheated water with high-pressure honey undergoes nucleation and carbonization process to create nano carbon-sphere (CS) [15]. The

3.1 Catalyst characterization

X-ray Diffraction (XRD) patterns CTF-1 and CS (Figure 3) showed a broad diffraction peak centered around 25.6^{O} signifying the amorphous or semi-crystalline nature of CTF-1, amorphous 2θ peak at 25.6^{O}, corresponding to the (002) plane of graphite structure. However, CS has more prominent 2θ peak at 43.6^{O} from (100) plane diffraction compared to CTF-1 [16]. The (100) plane of CS means the more prominent 3D crystalline properties compared to CTF which is more planar [17].

Fourier Transform Infrared Spectroscopy (FTIR) analysis (Figure 4) of CTFs further confirmed the successful formation of triazine rings. The spectra showed prominent peaks in the 1550–1600 cm^{-1} region, attributed to C=N stretching vibrations, and peaks between 1300–1400 cm^{-1}, associated with C–N stretching [18]. The CS has C=C bond peak at 1580 cm^{-1} as assigned to aromatic ring structure. C-H peak at 1133.5 cm^{-1} is also present on CS FTIR spectra [19].

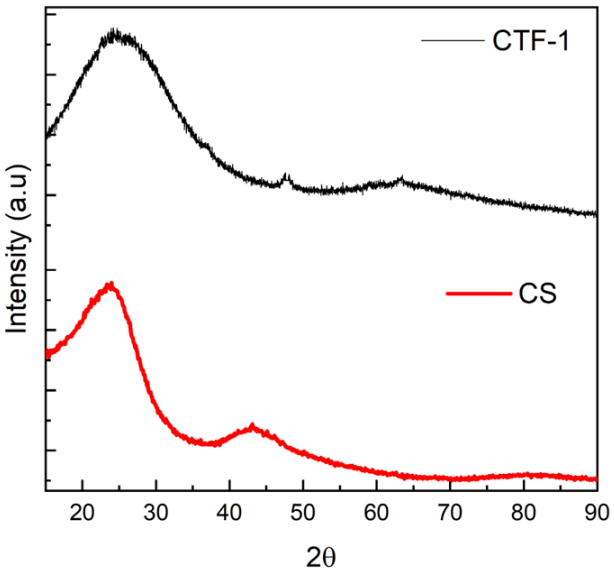

Fig. 3. XRD pattern of CTF-1 and CS

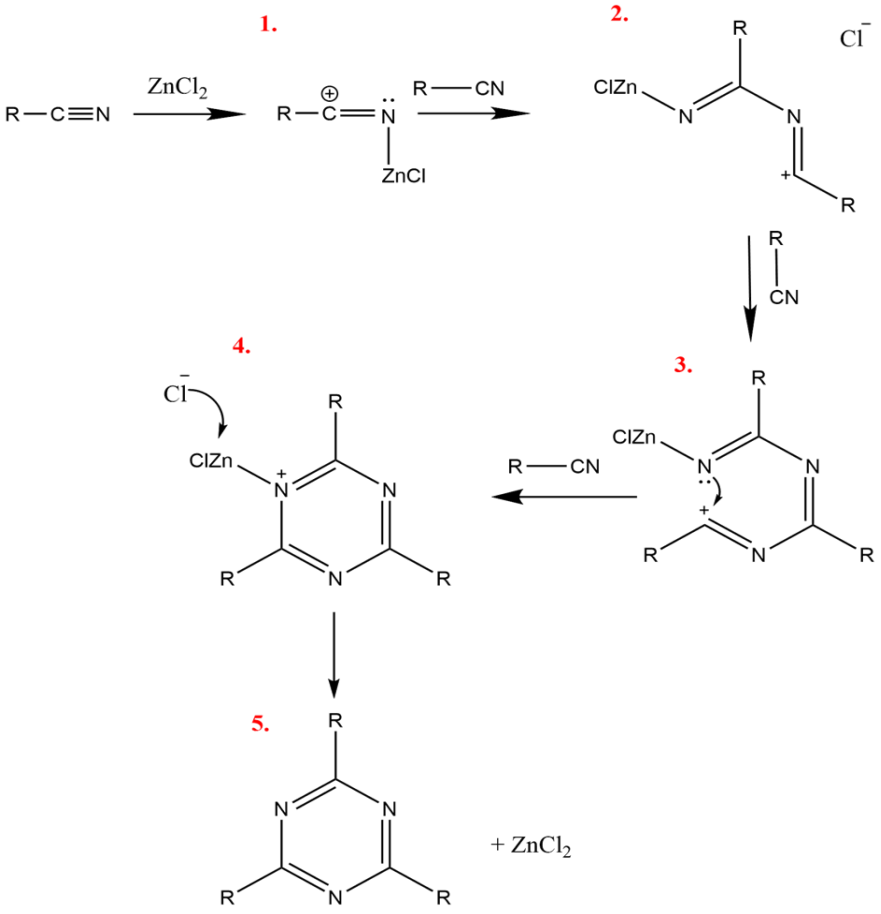

Fig. 2. CTF synthesis from DCB in ionothermal synthesis

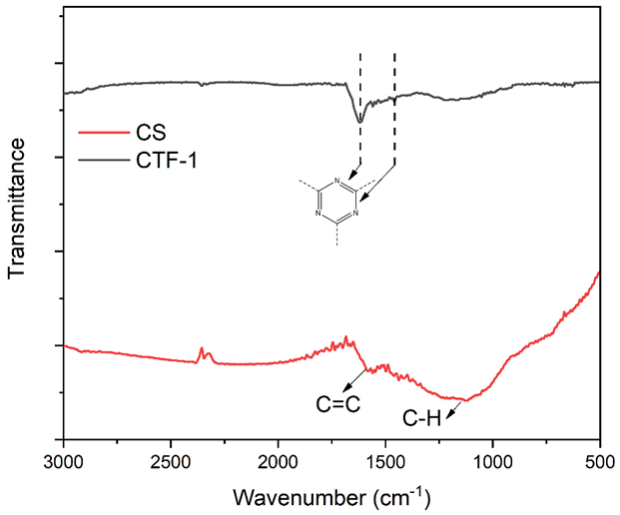

Fig. 4. FTIR Spectra of CTF and CS

The morphology of the CTFs material according to the FESEM image in Figure 5. CTF-1 have flake-like surface with the size of 2-5 µm. However, carbon nanosphere (CS) has spherical shape morphologies with a particle size distribution between 50 and 100 nm [20].

The nitrogen adsorption-desorption experiment was carried out to evaluate the surface area and porosity profile of the materials. CTF-1 as shown in Figure 6 shows typical type I BET isotherm with hysteresis loop. From the BET profile, CTF-1 could be described as nanoporous pore profile with 650 m^2/g of surface area [21]. The CS shows type V BET isotherm with H_3 loop isotherm [22]. It can be ascribed with mesoporous pore material properties. The CS has extremely high surface which is 1200 m^2/g.

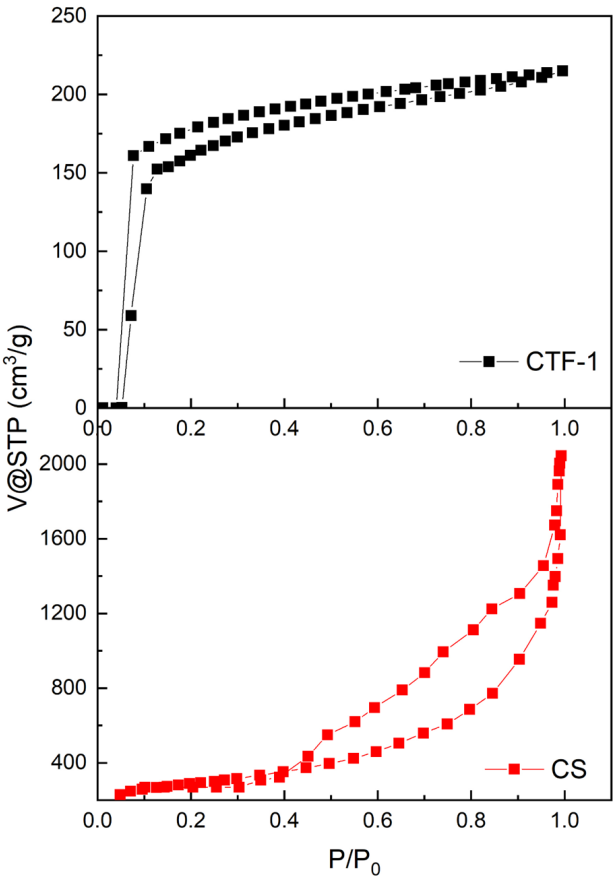

Fig. 6. N_2 adsorption and desorption isotherms of as-prepared catalysts CTF-1 and CS.

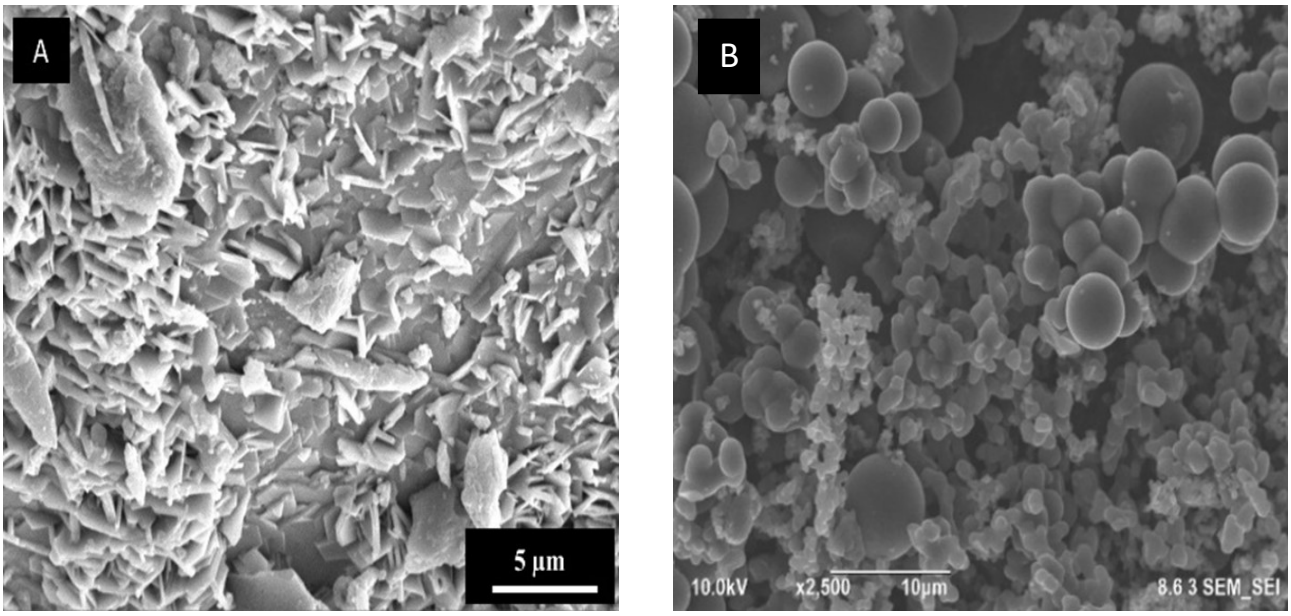

Fig. 5. SEM image of CTF-1 (A), CS (B)

The optical properties of the material using UV-Visible diffuse reflection spectra. As it can be seen, CS demonstrate absorption in the UV light range from 200-300 nm. CTF-1 on the other-hand, has broader of light absorption ranges from 200-476 nm [23, 24]. The broader range of light absorption from CTF-1, meaning CTF-1 could be use as active photocatalyst in the visible light area. On the other hand, CS has absorbed the light below 400 nm, which mean CS can only active in UV light range hindering the usage in low photon energy (e.g. sunray). Band gap value of the material can be calculated using Kubelka-Munk methods using the equation [25]:

$$\alpha h\nu = A(h\nu - E_g)^{\gamma} \quad (1)$$

where α, hν, γ, E_g, and A are the absorption constant, photon energy, natural electronic transition, band-gap energy (eV) and constant value relative to the semiconductive material. The Kubelka-Munk function could be plotted and could be linear-fitted to draw the band-gap size of the materials [26]. As the Figure 7 shows CTF-1 has smaller band-gap size (2.64 eV) compared to CS (3.5 eV). as it can be seen, smaller band-gap of CTF-1 make it more efficient in the photon-induced process since it has less energy requirement compared CS with the bigger bad-gap [27].

XPS analysis was further conducted to investigate the chemical properties of CTF-1. The C 1s spectrum of CTF-1 reveals two distinct peaks, as shown in Figure 8 (a). The first signal at 284.8 eV shows the corresponding peak of C=C from CTF-1 structure. The other peak, at 285 eV is corresponding to C=N from triazine unit. The N 1s spectra is done as shown in Figure 8 (b). the prominent peak at 401 eV correspond to N in triazine ring. The smaller peak at 402.eV could be assigned for graphitic N or N bonded to C without any active π-bond. The XPS study of the material shows that triazine functional group is present in the CTF-1 that successfully synthesized [17, 28, 29].

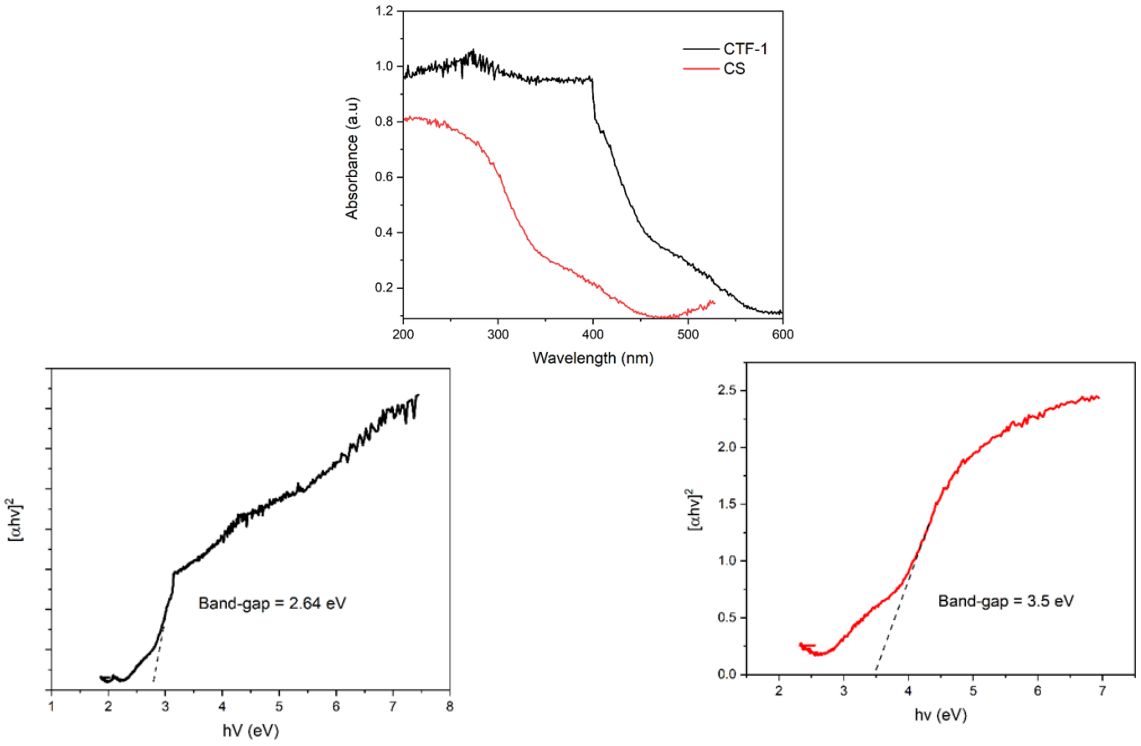

Fig. 7. UV-DRS absorption of CTF-1 and CS (A), Kubelka-Munk plot of CTF-1 (B), and CS (C)

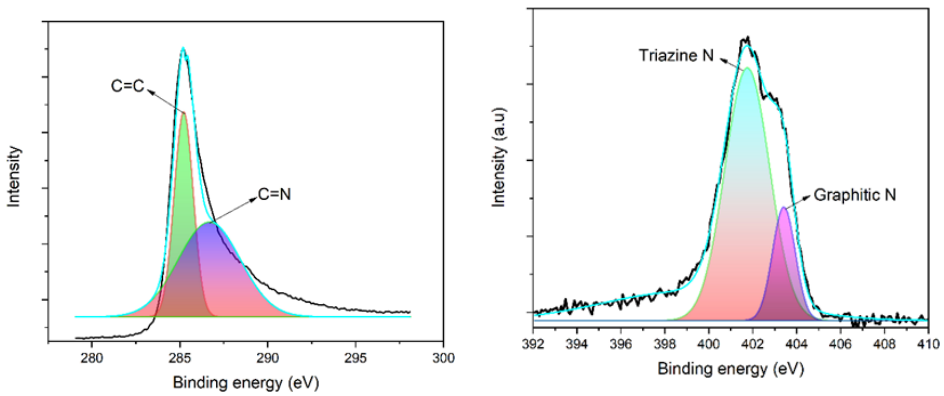

Fig. 8. XPS Spectra of CTF-1 C 1s (A), and N 1s (B)

3.2 Photo-Fenton catalytic degradation of MB

3.2.1 Preliminary study

The catalytic performance on the photo-Fenton degradation reaction of the both catalyst of CS and CTF-1 was investigated using MB dyes solution with concentration of 20 mg/L with the addition H_2O_2 2 mM as an oxidant in the photo-Fenton process to produce radicals needed in the degradation process. To quantify the degradation process, pseudo-first-order kinetic model is investigated using the equation [30]:

$$C_{MB} = C_{MB_0} e^{-k_{obs}t} \quad (2)$$

C_{MB} and C_{MB_0} are the MB concentration at initial time (t_0) and different time (t). the k_{obs} is pseudo-first-order constant calculated from degradation data. As seen, from the Figure 9, there was the difference in performance of CTF-1 and CS in the degradation of MB. CS has removal efficiency of 81.3 % with k_{obs} value of 0.0045 min^{-1} and CTF-1 with removal efficiency of 96.2 % with k_{obs} value of 0.027 min^{-1}. CS has lower efficiency compared to the CTF-1 in photo-Fenton reaction could be due of larger band-gap value of CS compared to CTF-1 (3.5 eV vs. 2.64 eV). Although CS known with high surface area which consider to active site to activate H_2O_2 into certain radicals, however with large band-gap of CS, the photocatalytic of radical producing process is not as efficient of CTF-1 with lower-band gap value. Lower band-gap make the electron movement from photon energy to have less energy requirements [31].

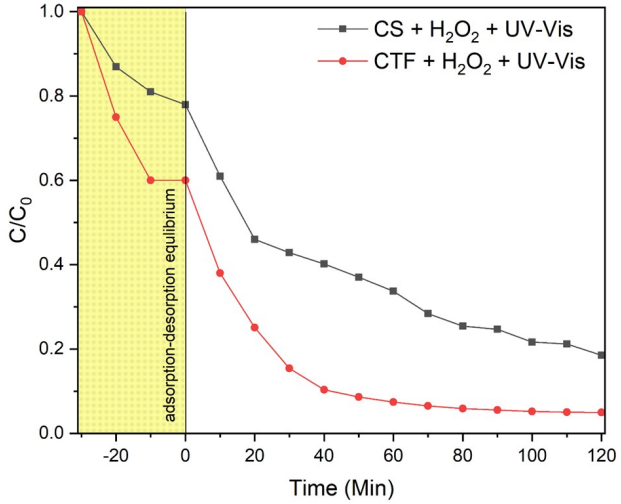

Fig. 9. comparison of the performance of CS and CTF-1 for photo-Fenton MB removal. (Condition of reaction $[MB_0]$ = 20 mg/L; $[H_2O_2]$ = 2 mM; Catalyst dosage 0.3 g/L.)

3.2.2 Different MB concentration study

Different MB concentration effect was tested using CTF-1 in photo-Fenton degradation reaction. The results of this study were displayed in Figure 10 The result of this study shows initial MB has significant effect on degradation. As it can be seen, as the higher MB concentration the degradation rate and efficiency were lower. At the lowest $[MB_0]$ = 10 mg/L the photo-Fenton efficiency is 98.4 % with k_{obs} of 0.0318 min^{-1}. At $[MB_0]$ = 20 mg/L the photo-Fenton efficiency is 96.2 % with k_{obs} of 0.0271 min^{-1} and for the $[MB_0]$ = 30 mg/L the photo-Fenton efficiency is 90.4 with k_{obs} of 0.0221 min^{-1}. Initial MB concentration affects the degradation process due the fact that higher concentration/quantity of dyes as reactant in photodegradation process also needs more oxidant to have the same amount degradation efficiency. Besides, higher MB concentration blocks partial photon energy towards catalyst surface, which make less energy available to move electron for radical production [32, 33].

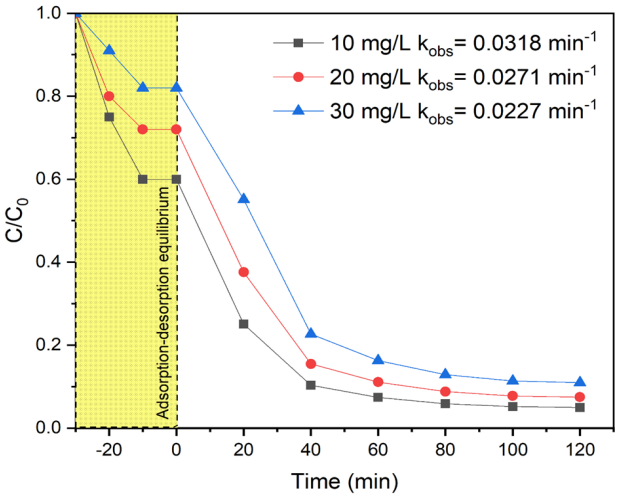

Fig. 10. comparison of the performance of CS and CTF-1 for photo-Fenton MB removal. (Condition of reaction $[MB_0]$ = 20 mg/L; $[H_2O_2]$ = 2 mM; Catalyst dosage 0.3 g/L.)

3.2.3 Reusability study of the catalyst

The stability and recyclability of the CTF-1 was conducted. As shown in Figure 11, the degradation efficiency of the CTF-1 after fourth usages is slightly reduced. The first, second, third, and fourth usage of the CTF-1 as photo-Fenton catalyst has the efficiency of 98.4 % (k_{obs} = 0.0318 min^{-1}); 95.4 % (k_{obs} = 0.0218 min^{-1}); 87.6 % (k_{obs} = 0.0182 min^{-1}); and 82.4 % (k_{obs} = 0.0081 min^{-1}) respectively. The slight decreased in photo-degradation of MB (< 20%) proves that CTF-1 has good stability in photo-Fenton reaction.

3.2.4 Degradation mechanism study

The mechanism of photo-Fenton degradation of CTF-1 was studied by scavenger study. The scavengers used were methanol as •OH scavenger, KI as h_{vb} scavenger, and $K_2Cr_2O_7$ as e_{cb} scavenger [34, 35]. Figure 12 shows MB degradation efficiency was affected by the addition of the scavengers. Methanol greatly affected the degradation efficiency, as the degradation efficiency only as 23 % of dyes removal with k_{obs} of 0.000018 min^{-1}. The addition of $K_2Cr_2O_7$ as e_{cb} scavenger in the MB degradation process reduce the degradation efficiency up to 50% into 48.4 % with k_{obs} of 0.00036 min^{-1}. The last scavenger added is KI for h_{vb} scavenger however, only 10 % of degradation efficiency affected, as the overall degradation efficiency is 88.4 % with k_{obs} = 0.0081 min^{-1}. The scavenger study shows that the photo-Fenton degradation of CTF-1 affected by •OH radical and e_{cb}.

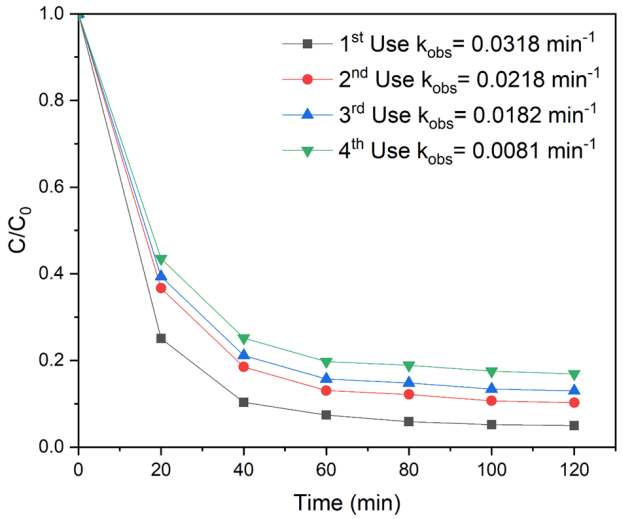

Fig. 11. Recyclability of the CTF-1 on photo-Fenton degradation of CTF-1. (Condition of reaction [MB_0] = 10 mg/L; [H_2O_2] = 2 mM; Catalyst dosage 0.3 g/L.)

As it has known, the photo-Fenton reaction utilizes •OH radical produced from H_2O_2 as oxidant precursor. The •OH radical production from H_2O_2 in photo -Fenton reaction using semiconductive catalyst usually happened in three steps [36];

1. Absorption of photon energy on the catalyst surface
2. Charge separation and migration on the surface of the catalyst
3. Surface redox reaction to produce radicals.

The scavenger studies shown that MB degradation in this study was greatly affected by •OH radicals and e_{cb} species, yet h_{vb} is the minor species. The schematic reaction of MB degradation by photo-Fenton process is [19, 36, 37], the mechanism of the process is shown in Figure 13 :

$$CTF\text{–}1 + h\nu \rightarrow CTF\text{–}1\ (h^+ + e_{cb}) \quad (3)$$
$$e_{cb} + H_2O_2 \rightarrow 2\ \bullet OH \quad (4)$$
$$h_{vb} + H_2O_2 \rightarrow O_2 + 2H^+ \quad (5)$$
$$e_{cb} + O2 \rightarrow o_2^- \quad (6)$$
$$h_{vb}/\bullet OH/o_2^- + Dyes(MB) \rightarrow H_2O + CO_2 + \text{intermediates} \quad (7)$$

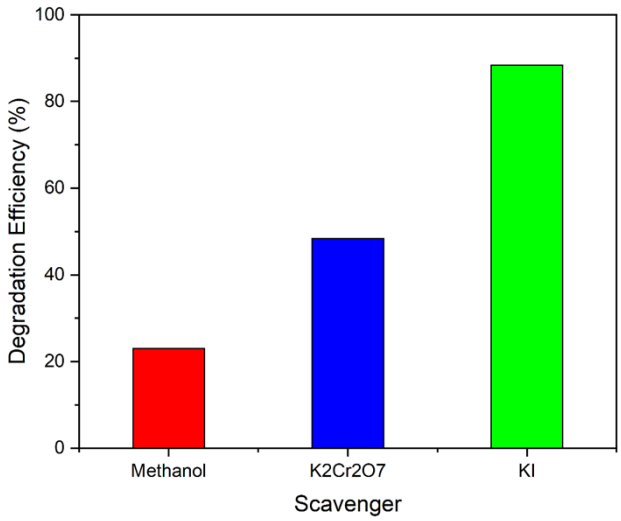

Fig. 12. Scavenger study of the CTF-1 on photo-Fenton degradation of CTF-1. (Condition of reaction [Methanol; $K_2Cr_2O_7$; KI] = 2 mM; Catalyst dosage 0.3 g/L.)

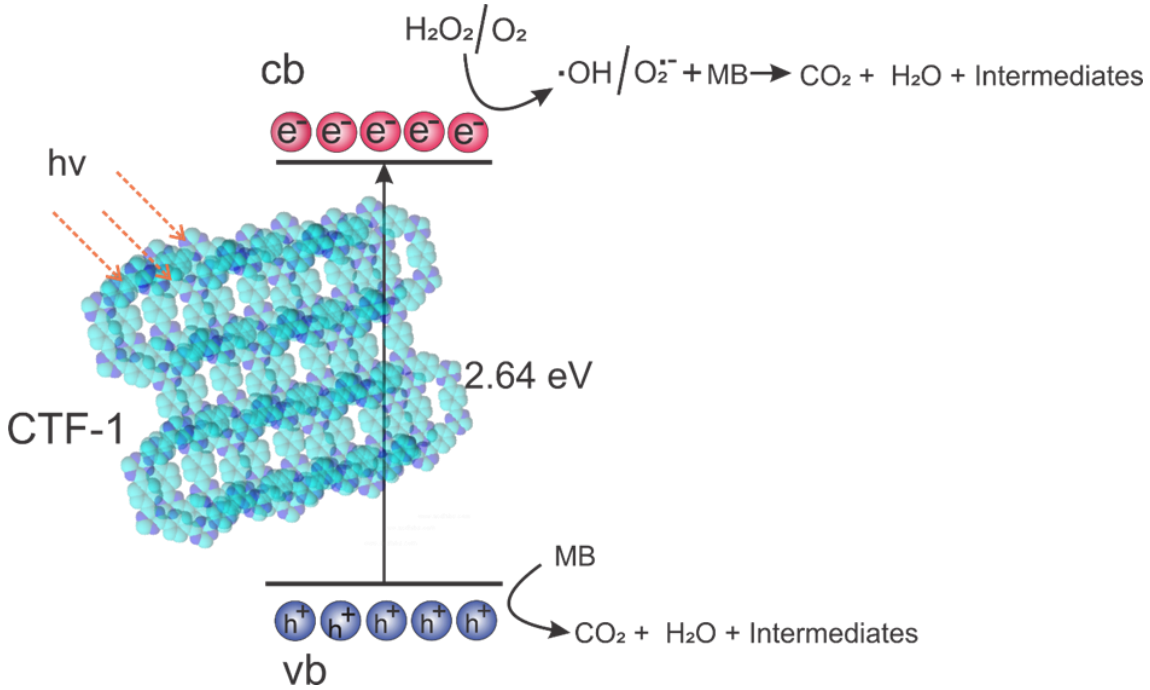

Fig. 13. XPS Spectra of CTF-1 C 1s (A), and N 1s (B)

4. CONCLUSION

Two carbon-based catalysts, namely CTF-1 and CS were successfully synthesized. Carbon-based catalyst with less inorganic properties meaning more environmentally friendly to be used in pollutant removal and environmental remedies. In this study CTF-1 was synthesized using ionothermally, meaning no harmful solvent is used as well as CS that synthesized using hydrothermal methods. Both of the materials then used in photo-Fenton degradation reaction of MB. The results shows that CTF-1 has better degradation efficiency compared to CS due CTF-1 has smaller band-gap value. Smaller band-gap value in CTF-1 makes the charge separation and migration process faster with the same amount of photon energy. Photo-Fenton mechanism of CTF-1, proved that •OH and e_{cb} are the main active species in the degradation reaction. This study shows that non-metal materials, CTF-1, could be used as photo-Fenton catalyst since with the help of photon energy, it could produce active radicals to degrade the organic pollutant.

AUTHOR INFROMATION

Corresponding Author
*Email: barata.aditya5610@student.unri.ac.id

ORCID

Barata Aditya Prawiranegara : 00000-0003-0023-8492
Heni Sugesti : 00009-0003-6069-5334
Hussein Rasool Abid : 00000-0003-3368-371X
Muhammad Rizwan Azhar : 00000-0002-5938-282X
Maykel Manawan : 00000-0003-3782-1307
Panca Setia Utama : 00000-0002-6829-1321

REFERENCES

[1] Ahmed, B., et al., Photo-Fenton treatment of actual agro-industrial wastewaters. Industrial & Engineering Chemistry Research, 2011. 50(11): p. 6673-6680.
[2] Zazouli, M.A., et al., Municipal solid waste landfill leachate treatment by fenton, photo-fenton and fenton -like processes: Effect of some variables. Iranian journal of environmental health science & engineering, 2012. 9: p. 1-9.
[3] López, J.C., et al., Integration of solar photocatalysis and membrane bioreactor for pesticides degradation. Separation Science and Technology, 2010. 45(11): p. 1571-1578
[4] Lucas, M.S., et al., Solar photochemical treatment of winery wastewater in a CPC reactor. Journal of Agricultural and Food Chemistry, 2009. 57(23): p. 11242-11248.
[5] Ballesteros Martin, M., et al., An analysis of the bacterial community in a membrane bioreactor fed with photo-Fenton pre-treated toxic water. Journal of Industrial Microbiology and Biotechnology, 2011. 38 (9): p. 1171-1178.
[6] Xue, Z., et al., Degradation of tetracycline with BiFeO3 prepared by a simple hydrothermal method. Materials, 2015. 8(9): p. 6360-6378.
[7] Metin, S. and D.İ. Çifçi, Chemical industry wastewater treatment by coagulation combined with Fenton and photo-Fenton processes. Journal of Chemical Technology & Biotechnology, 2023. 98(5): p. 1158-1165.
[8] Fu, J., et al., Mass Transfer-Enhanced Photothermal Membranes with Synergistic Light Utilization for High -Turbidity Wastewater Purification. Angewandte Chemie International Edition, 2025. 64(11): p. e202421800.
[9] Agustina, T.E., et al., Laboratory wastewater treatment by using combination methods of AOPs and chemical-physical pretreatments. Ecological Engineering & Environmental Technology, 2024. 25.
[10] Guzmán, J., et al., Combined photo-fenton–SBR processes for the treatment of wastewater from the citrus processing industry. Journal of Agricultural and Food Chemistry, 2015. 63(2): p. 391-397.
[11] Imran, N.J. and M. Al-Furaiji, Comparison of TiO2 Thin Film Photocatalytic and Enhanced Photo-Fenton's Detector for Wastewater Treatment from Power Plants. ChemistrySelect, 2025. 10(17): p. e202500366.
[12] Freitas, A., et al., Ecotoxicity evaluation of a WWTP effluent treated by solar photo-Fenton at neutral pH in a raceway pond reactor. Environmental Science and Pollution Research, 2017. 24: p. 1093-1104.
[13] Aslam, T., et al., Valorization of acid mine drainage into an iron catalyst to initiate the solar photo-Fenton treatment of municipal wastewater. Environments, 2023. 10(8): p. 132.
[14] Rangaraj, V.M., K.S.K. Reddy, and G.N. Karanikolos, Ionothermal synthesis of phosphonitrilic-core covalent triazine frameworks for carbon dioxide capture. Chemical Engineering Journal, 2022. 429: p. 132160.
[15] Li, M., W. Li, and S. Liu, Hydrothermal synthesis, characterization, and KOH activation of carbon spheres from glucose. Carbohydrate research, 2011. 346(8): p. 999-1004.
[16] Tai, F., et al., Raman and X-ray diffraction analysis on unburned carbon powder refined from fly ash. Journal of Raman Spectroscopy, 2010. 41(9): p. 933-937.
[17] Pourebrahimi, S., et al., Synthesis, characterization, and gas (SO2, CO2, NO2, CH4, CO, NO, and N2) adsorption properties of the CTF-1 covalent triazine framework-based porous polymer: experimental and DFT studies. Journal of Porous Materials, 2024. 31 (2): p. 643-657
[18] He, X., et al., Exploration of 1D channels in stable and high-surface-area covalent triazine polymers for effective iodine removal. Chemical Engineering Journal, 2019. 371: p. 314-318.
[19] Saputra, E., et al., High performance magnetic carbonaceous materials as a photo Fenton-like catalyst

for organic pollutant removal. Journal of Water Process Engineering, 2022. 47: p. 102849.
[20] Mi, Y., et al., Synthesis of carbon micro-spheres by a glucose hydrothermal method. Materials Letters, 2008. 62(8): p. 1194-1196.
[21] Lee, Y.J., S.N. Talapaneni, and A. Coskun, Chemically activated covalent triazine frameworks with enhanced textural properties for high capacity gas storage. ACS applied materials & interfaces, 2017. 9(36): p. 30679-30685.
[22] Chang, B., et al., Convenient synthesis of porous carbon nanospheres with tunable pore structure and excellent adsorption capacity. Journal of Hazardous Materials, 2013. 262: p. 256-264.
[23] Li, L., et al., Band-gap engineering of layered covalent organic frameworks via controllable exfoliation for enhanced visible-light-driven hydrogen evolution. International Journal of Hydrogen Energy, 2020. 45 (4): p. 2689-2698.
[24] Hayat, A., et al., Emerging breakthroughs in covalent triazine frameworks: From fundamentals towards photocatalytic water splitting and challenges. Progress in Materials Science, 2025. 147: p. 101352.
[25] Landi, S., et al., Use and misuse of the Kubelka-Munk function to obtain the band gap energy from diffuse reflectance measurements. Solid State Communications, 2022. 341: p. 114573.
[26] George, P. and P. Chowdhury, Complex dielectric transformation of UV-vis diffuse reflectance spectra for estimating optical band-gap energies and materials classification. Analyst, 2019. 144(9): p. 3005-3012.
[27] Gao, S., et al., Band Gap Tuning of Covalent Triazine-Based Frameworks through Iron Doping for Visible-Light-Driven Photocatalytic Hydrogen Evolution. ChemSusChem, 2021. 14(18): p. 3850-3857.
[28] Shao, L.-H., et al., Constructing tightly integrated conductive metal-organic framework/covalent triazine framework heterostructure by coordination bonds for photocatalytic hydrogen evolution. Journal of Colloid and Interface Science, 2023. 633: p. 233-242.
[29] Hu, X., et al., Crystalline covalent triazine frameworks manipulated by aliphatic amine modulator. Science China Chemistry, 2023. 66(9): p. 2676-2682.
[30] Wu, C.-H. and J.-M. Chern, Kinetics of photocatalytic decomposition of methylene blue. Industrial & engineering chemistry research, 2006. 45(19): p. 6450-6457.
[31] Marcelino, R.B. and C.C. Amorim, Towards visible-light photocatalysis for environmental applications: band-gap engineering versus photons absorption—a review. Environmental Science and Pollution Research, 2019. 26: p. 4155-4170.
[32] Ahmed, Y., Z. Yaakob, and P. Akhtar, Degradation and mineralization of methylene blue using a heterogeneous photo-Fenton catalyst under visible and solar light irradiation. Catalysis Science & Technology, 2016. 6(4): p. 1222-1232.
[33] Liu, Y., et al., Enhanced catalytic degradation of methylene blue by α-Fe2O3/graphene oxide via heterogeneous photo-Fenton reactions. Applied Catalysis B: Environmental, 2017. 206: p. 642-652.
[34] Lou, W., et al., Study of a photocatalytic process for removal of antibiotics from wastewater in a falling film photoreactor: Scavenger study and process intensification feasibility. Chemical Engineering and Processing: Process Intensification, 2017. 122: p. 213-221.
[35] Schneider, J.T., et al., Use of scavenger agents in heterogeneous photocatalysis: truths, half-truths, and misinterpretations. Physical Chemistry Chemical Physics, 2020. 22(27): p. 15723-15733.
[36] Lin, J., et al., Functional carbon nitride materials in photo-Fenton-like catalysis for environmental remediation. Advanced Functional Materials, 2022. 32 (24): p. 2201743.
[37] Zhu, C., et al., Insights into excitonic behavior in single-atom covalent organic frameworks for efficient photo-Fenton-like pollutant degradation. Nature Communications, 2025. 16(1): p. 790.